Daily Integrity Checks Using Automated DFR's Records Analysis

Claude Fecteau* Denis Larose Raymond Bégin Jean-Guy Lachance

Hydro-Québec

Abstract: *This paper proposes a novel approach to improve the reliability of the Digital Fault Recorder (DFR) systems by forcing a recording daily and performing automatically some integrity checks on the measurements. These checks also aim to detect some latent failures in the power apparatus and to report abnormal network conditions earlier. The paper describes how this philosophy has been put into practice at Hydro-Québec last year. The paper presents the system architecture and describes the signal processing functions implemented to achieve the goals. After just a few months of operation, the approach proved to be very effective and some early results are given. It is also proposed to extend this approach by cross-checking the redundant measurements against other Intelligent Electronic Devices (IEDs) such as the digital relays and the Phasor Measurement Units (PMUs) for instance. The synergy created in this way should permit to increase the availability and integrity of each of those systems. It is also expected that the early detection of hidden failures will contribute to improve the reliability of the power systems.*

I. Introduction

The Digital Fault Recorders (DFRs) are very useful for the post event analysis following a power system disturbance. Most regulation organizations require that the utilities maintain such devices to help the reconstitution of the sequence of events in case of a blackout. The DFRs are also of great value to investigate the behaviour of the protective relays. Moreover, they can be used for fault location on transmission lines. Some distinctive characteristics of the Hydro-Québec's network are presented in section II to explain its great interest for this particular application. Many years of experience revealed however some reliability issues with the DFR system and some causes for errors are given. An approach is proposed in section III to improve its reliability. Basically, a trigger is forced regularly to all the DFRs and some automated integrity checks are performed on the measurements. This concept has been put into practice last year and the architecture of the system supporting it is illustrated. Different kinds of integrity checks are applied depending whether the signals are classified in a steady-state or a transient-state and a method is proposed to discriminate between them. The integrity checks suggested for the steady-state and the transient-state cases are presented in sections IV and V respectively. Some real-life examples are given of measurement errors detected automatically when applying these rules. It is also shown how the proposed approach can detect latent failures in the power apparatus and reveal power quality problems. In section VI, it is proposed to extend the approach by cross-checking the measurements against other IEDs, as the digital relays and the PMUs for instance.

*Contact information: fecteau.claude@ireq.ca
IREQ, 1800 boul. Lionel-Boulet, Varennes, Québec, Canada, J3X 1S1

II. Reliability issues with the DFR system

II.1 Hydro-Québec's experience with fault location using DFRs

Hydro-Québec undertook a vast program to replace its light beam oscillographs by digital fault recorders in the beginning of the nineties. Today, 184 DFRs are installed and 130 of them monitor near 600 ends of transmission lines. This technology shift permitted the automatic transmission of the records to a central location and their computerized processing. The time to transmit the records to the central office has been reduced from days, with the old photo-sensitive paper rolls, to a few minutes with the new digital format over telecommunication links. These new capabilities have motivated the start of an R&D project to develop and implement single-ended and double-ended fault location algorithms [1]. This application is particularly important to Hydro-Québec considering that the transmission lines cover about 30,000 km and the longest ones may cover over 400 km mostly in uninhabited area. The experience with the fault location algorithms over the years showed a very good overall performance. As a figure of merit, the error of the estimate is within 5% of the line length in the vast majority of the cases. This also applies for the original algorithms that were specifically developed to solve the complicated problem of estimating a fault location on series compensated lines. The total length of these lines at the 735 kV voltage level amounts to about 8,000 km. However, some faults couldn't be located accurately the first time. The searches for the root cause of a wrong result are very time consuming because there are so many possibilities for errors. It can be due to bad signals, an error in the line parameters, a limitation of the single-ended algorithm for highly resistive faults or a software bug. Sometimes the source of the error was only found months or even years later quite by chance. Most of the time however, the error could be attributed to the DFR system. By DFR system it is meant all the measuring process from the PTs and the CTs up to the final record received at the central server. This fact raised the need to improve its reliability. The need was further emphasized when it was planned to send the fault location estimate automatically to the field personnel by email in 2005. The whole process from the moment that the fault occurs to the mailing of the message would then be executed automatically without any human intervention or validation.

II.2 Sources of errors

The Table I resumes some of the errors belonging to the DFR system that were revealed by the fault location application. The first six errors concern the availability of the DFR system and these are not recoverable. Other errors concern the integrity and the quality of the measurements and their effect can be detrimental to the accuracy of the fault location estimate ("garbage in, garbage out!"). For example a

fault, which occurred on a 735 kV series compensated line, had not given any result on the line but the algorithm sensed the fault to be in the reverse direction. After careful examination of the signals, it was found that the polarity of all the currents of the DFR did not respect the convention. After multiplication by –1 to re-invert them, the algorithm located the fault caused by a broken guy-wire the next span from the exact location on this line 275 km long.

TABLE I: Errors found within the DFR system

DFR shutdown
DFR out for maintenance
DFR did not triggered
DFR lost record
DFR's memory full
DFR's hardware failure
DFR could not transmit
Loose contact
Corrupted record
Software bug
Bad or missing signals
Wrong signal assignment
Wrong phase rotation
Calibration error
PT or CT error
Wrong PT or CT ratio
Scaling error (bad units, rms vs crest value…)
Inverted polarity
Full scale exceeded
Bad grounding practice
Time stamp error

III. Improving the reliability of the DFR system

III.1 Forcing a recording to all the DFRs each day

Owing to the reliability concerns stated previously about the DFR system, an R&D project was started at the end of 2002 aiming to detect most of the errors automatically. The key idea driving the new approach is to force a recording regularly to all the DFRs then transmit the records to a central server, which would then perform some integrity checks automatically. It was chosen to trigger the DFRs every night because there is less switching actions on the network and the burden is lower on the communication links. An immediate benefit of this procedure is the detection of the DFRs that are not operational or could not transmit their record. This sole advantage has the greatest impact to improve the availability of the DFRs. On a longer term, it is also possible to compile statistics about the availability and tell precisely when a particular DFR transmitted a record for the last time. This information provides a clear overall picture about the availability of the DFRs to the management and permits to prioritize the maintenance effort.

III.2 Hydro-Québec's DFR system architecture

The figure 1 illustrates the overall DFR system architecture supporting the proposed approach as implemented at Hydro-Québec. Many components are common with the fault location application and this has permitted to put the system into service in a very short delay.

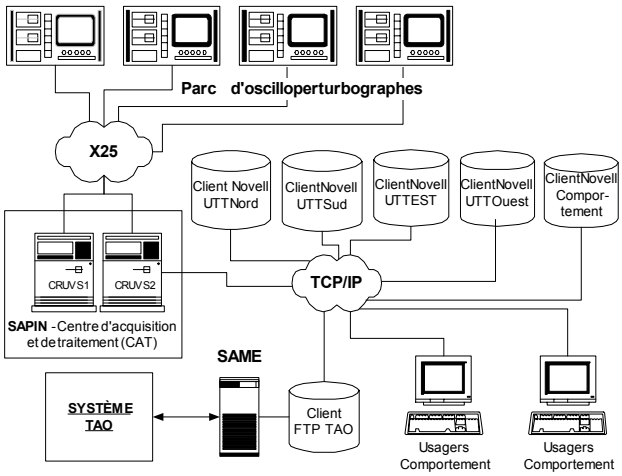

Figure 1: Overall system architecture

The figure 2 shows a simplified functional diagram of the system. The incoming records are stored on different directories whether the DFR has been forced to trigger or it triggered by itself when a disturbance was detected. The 'SAME' expert system accesses these records and calls the integrity check functions developed in Matlab. It produces reports and sends out email to those interested as necessary. The results are archived in an Oracle database and there is the possibility to compile statistics and perform some trend analysis. There is also an exchange of information with the 'MAXIMO' database used for the maintenance of the equipments.

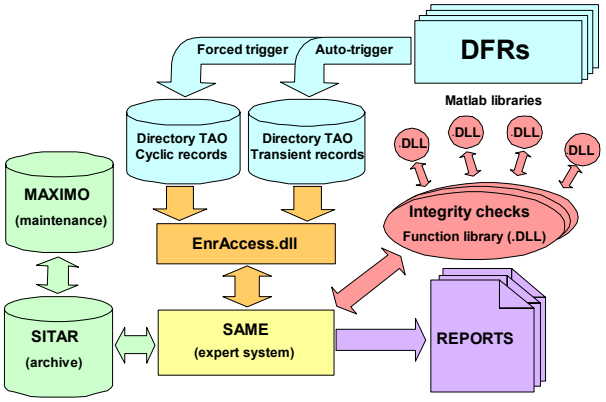

Figure 2: Functional diagram

III.3 Frequency domain analysis

The signals are classified as being in *steady-state* or in *transient-state*. The classification is performed by a signal analysis in both frequency and time domains. After appropriate filtering and resampling, a Discrete Fourier Transform (DFT) over a one cycle sliding window extracts the DC offset component, the fundamental component and the 2nd to 20th harmonics. Then each signal is classified in transient-state if the percentage of variation of the fundamental component exceeds a given threshold. The figure 3 illustrates a current signal and the variation of its fundamental component against the specified threshold.

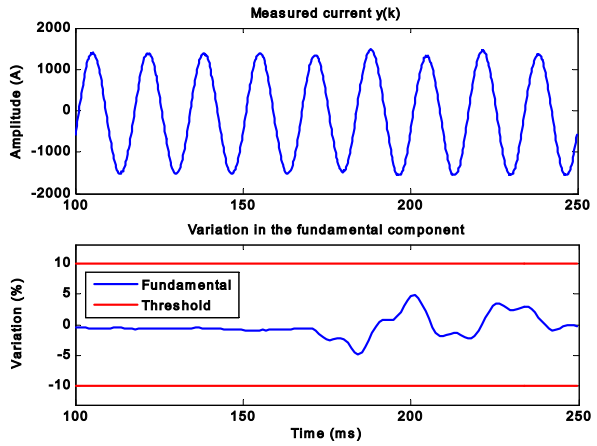

Figure 3: Variation in the fundamental component

III.4 Time domain analysis

An analysis is also performed in the time domain aiming to detect transient component into the signals. These components could remain unnoticed after the classification in the frequency domain because of the filtering effect of the DFT. Let $y(k)$, $k=1,...N$ be the digital sampled version of a time continuous signal $y(t)$ sampled at a rate of F_S Hz. The application of the superposition principle permits to express a general model of the signal $y(k)$ as the sum of a steady-state component $ss(k)$ and a transient component $tr(k)$:

$$y(k) = ss(k) + tr(k) \quad (1)$$

A model of the steady-state component can be represented as the sum of a DC offset, a fundamental component $(h=1)$ and harmonics $(h=2, 3, ..., H)$, where h is the rank of the harmonic:

$$ss(k) = DC + \sum_{h=1}^{H} A_h \cdot sin(\omega_h \cdot k / F_S + \theta_h) \quad (2)$$

The DC offset, the amplitudes A_h and the angles θ_h are the mean values of the parameters that have been computed previously by the sliding DFT. The highest harmonic H is limited by the Nyquist frequency, which is half the sampling rate. The transient component $tr(k)$ can then be obtained from (1) as the difference between the measured signal $y(k)$ and the computed steady-state component $ss(k)$:

$$tr(k) = y(k) - ss(k) \quad (3)$$

The signal is classified in a transient-state if an instantaneous transient value $tr(i)$ expressed as a percentage of the fundamental component A_1 exceeds a threshold T:

$$100 \cdot \left| \frac{tr(i)}{A_1} \right| > T(\%) \quad (4)$$

For computational efficiency in practice, the highest harmonic H can be chosen lower than half the sampling rate. For a DFR with Fs = 4800 Hz typically in use at Hydro-Québec, the 20th harmonic is chosen instead of the 40th. The higher harmonics should be negligible and even reduced by the low-pass anti-aliasing filter of the DFR. Otherwise, they will be reflected in the transient component of the signal, which is not dramatic because such high harmonics would then be confused with large noise and the signal would be classified in a transient-state.

Figures 4a and 4b illustrate the application of this analysis with real-life measurements. The upper part of figure 4a shows that a sound line voltage measurement $y(k)$ is indistinguishable from its computed steady-state component $ss(k)$ when they are superposed. The lower part of the figure shows that the corresponding computed transient component $tr(k)$ remains well below the specified threshold. On the other hand, the upper part of figure 4b illustrates a corrupted voltage measurement of another line taken from the same record. The lower part of the figure shows how the notches make the transient component to greatly exceed the threshold. A similar anomaly was also found on a line's neutral current in the same record. The common cause was attributed to a bad contact between a card's edge connector and the backplane of the DFR. It is worth mentioning that both hidden anomalies were detected automatically with the proposed approach.

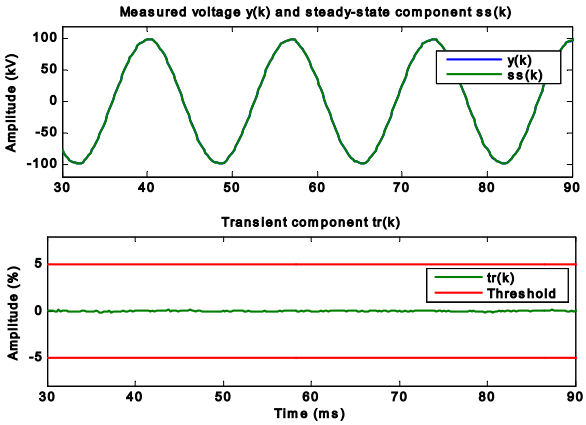

Figure 4a: Sound voltage measurement

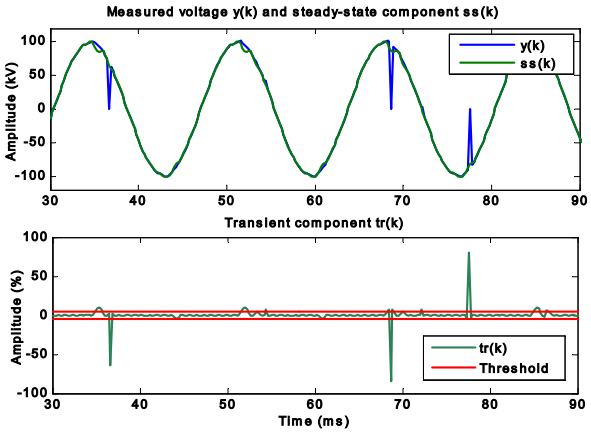

Figure 4b: Intermittent notches on voltage measurement

Figures 5 and 6 illustrate two more examples of corrupted voltage measurements that were detected automatically. The causes for these anomalies are not known as yet.

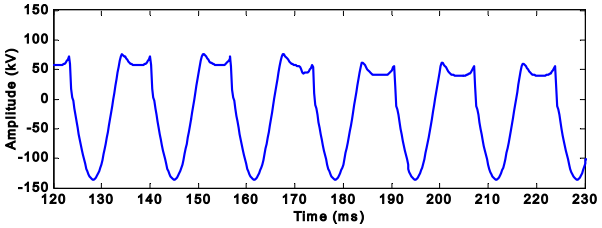

Figure 5: Distorted waveform of a voltage measurement

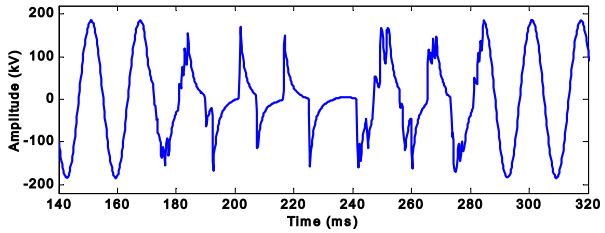

Figure 6: Intermittent error on a voltage measurement

When all the signals are classified as steady-state or transient-state, an empirical rule is applied to discriminate between a transient occurring on the power network and an erroneous transient component in the signal.

IV. Steady-state integrity checks

This section proposes some integrity checks that apply to steady-state measurements. Many steady-state parameters are computed and checked against thresholds. These are presented first then many consistency checks are described next.

IV.1 Checking steady-state parameters

The steady-state parameters that are computed are divided into four categories as follows:

Mean bus voltages (for each bus)
- Mean symmetrical components (V_0, V_1, V_2)
- Mean percentage of unbalance (V_2/V_1)
- Mean module and phase (per phase)
- Mean Total Harmonic Distortion (per phase)

Three phase line currents (for each line)
- Symmetrical components (I_0, I_1, I_2)
- Percentage of unbalance (I_2/I_1)

Single phase voltages (for each bus and each line)
- Module and phase of the fundamental component
- Difference between the mean voltage for the bus
- DC Offset
- Harmonics 2nd to 20th
- Total Harmonic Distortion (THD)

Single phase line currents (for each line)
- Module and phase of the fundamental component
- DC Offset
- Harmonics 2nd to 20th
- Total Harmonic Distortion (THD)

It should be noted that there is five currents considered for each line in the implemented version at Hydro-Québec. They are the three line currents, the neutral current of the line and the neutral current of the shunt inductances when present.

In addition to these parameters, the frequency is computed for each valid voltage then the mean value and the standard deviation are determined. Each steady-state parameter is checked against a specific threshold to make sure it remains within normal values. This represents an extensive checking if we consider for example that a DFR, which monitors the voltages and currents of three lines in addition to a three phase bus voltage, would implicate the checking of 590 parameters. An abnormal value of a parameter could be the sign of power quality problems like excessive unbalance or harmonics and can also reveal errors in the measurement process. Table II gives many examples of coarse errors on the line current measurements and their effect on the symmetrical components.

TABLE II: Coarse errors on three phase currents and their effects on the symmetrical components

Type of error	I_0 (p.u.)	I_1 (p.u.)	I_2 (p.u.)	Unbalance I_2/I_1
Sound signals (no error)	0	1	0	0 %
Permutation *bca* or *cab*	0	1	0	0 %
Permutation *acb*, *bac* or *cba*	0	0	1	n.d.*
One null signal	1/3	2/3	1/3	50 %
Two null signals	1/3	1/3	1/3	100 %
Three null signals (trivial)	0	0	0	n.d.
One signal inverted	2/3	1/3	2/3	200 %
Two signals inverted	2/3	1/3	2/3	200 %
Three signals inverted	0	1	0	0 %

*Not defined

The figure 7 presents a real-life example of current measurements recorded during a fault on a line. The upper part of the figure shows the faulted phase A current of the line L1 superposed over the phase A current of a parallel line L2. Both currents coincide well in the prefault period as expected. However, the lower part of the figure shows that the prefault current of the sound phase C of line L1 is quasi null before the fault occurs and then it suddenly matches the phase C current of line L2 afterwards. One null signal induces an apparent unbalance as shown in Table II. This error was recovered by copying the prefault current of the phase C of line L2 and pasting it to the prefault portion of the phase C of line L1 in order to obtain a better fault location estimate. The strange behaviour of the current was later attributed to a loose connection. This error would have been caught earlier with the proposed daily integrity checks.

The Table II shows that there are some errors like a circular permutation 'bca' or 'cab' and when three signals are inverted that can't be discriminated from sound signals with the symmetrical components. One must then compare the signals with other redundant measurements or make some assumptions about the direction of the load flow to be able to detect these kinds of error. Some solutions are given next for various cases.

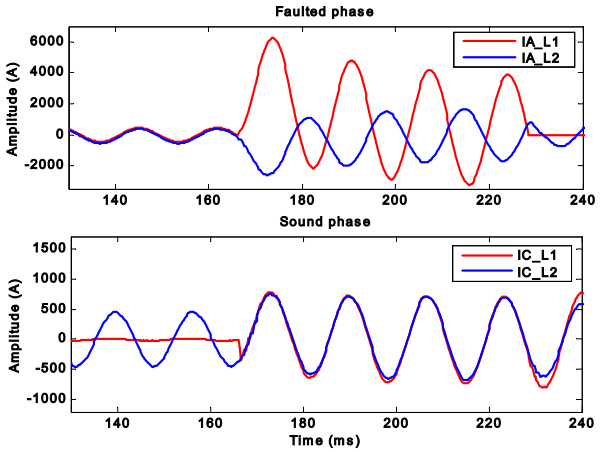

Figure 7: Corrupted prefault current on one parallel line

IV.2 Line current measurement checks

No redundancy is usually available with the line current measurements. However, there are particular cases where some validations are still possible. If a significant error is present on a current measurement, it could be caught if it induces an unbalance exceeding a given threshold. Otherwise, if many parallel lines join the same two terminals and no tap is present, it is possible to compare all the currents of the same phase against each other. The superposition on the same graphic of the prefault current measurements of two parallel lines has once before permitted to find quite by chance a circular permutation 'bca' on the unfaulted line. The checking between the currents of parallel lines has also permitted to explain why the one-ended fault location algorithm couldn't locate a fault on a 735 kV line 375 km long. The comparison of the prefault currents with two other parallel lines revealed an error in the specified CT ratio that was half the correct value. After having corrected the error, the estimate obtained was at 2.5 km of the defective insulator string that caused the short-circuit. If the current measurements are available at both ends of a line then these sorts of gain error can be detected without the need for parallel lines when applying the end-to-end checks explained further. Other kind of current measurement checks are also possible by verifying for instance that all the currents going in and out of a given apparatus respect the Kirchoff's current law. The same principle can be applied at all time to the three phase currents of a transmission line and it's neutral current which must add up to a value close to zero. This kind of check is discussed in more detail in section V.

IV.3 Redundant voltage measurement checks

The line voltages and the bus voltages usually provide redundant measurements. If the line's PT is on the line side relative to the breaker, then one must ensure that the line is closed at the local end to measure the bus voltage. This can be asserted by verifying that the corresponding line current exceeds a minimum value. A mean bus voltage can then be computed against which each voltage measurement is compared. The voltage difference represents one of the single phase voltage steady-state parameter that is daily checked against a threshold.

This checking has already permitted to find automatically some PTs that presented an abnormal drift. Such error has deteriorated the fault location estimate in a few cases in the past. Since the protective relays are tied to the same PTs, the early detection of these hidden failures contributes to reduce the risk of a misoperation. An example of this was experienced when a shunt capacitor was repeatedly switched off because a magnetically coupled voltage transformer was giving a voltage too high. The capacitive coupling voltage transformer (CCVT) seems also to be prone to drift when some capacitors in the divider side deteriorate and end up short-circuited. A difference up to 18% has been observed in the past on a defective CCVT and it was then necessary to replace it urgently. Such a difference should be indeed taken seriously because there is a potential risk for a catastrophic failure when the remaining capacitors get subjected to higher voltages. The proposed approach allows precisely making an automatic follow up of this difference daily and performing some trend analysis. It is not possible however to determine whether the source of an error comes from the PT or the DFR system. When a significant error is pointed out then a technician is called for verifying the input signals of the DFR. The automatic discrimination of the source of the error would be nevertheless possible by cross-checking the DFR's measurements against other independent measurements taken by various IEDs as discussed further in section VI.

IV.4 End-to-end checks

When two DFRs monitor both ends of a transmission line it is possible to perform end-to-end checks provided that both records overlap in time. This overlapping is necessary to prevent wrong deductions if the network conditions change between the measurements. The processing of the remote forced trigger command is not executed in a sufficiently precise deterministic time to guarantee this overlapping with the present implementation at Hydro-Québec. It would be useful if a command could be sent to the DFRs asking for an auto triggering at a prescribed instant given by their synchronized clock. Despite this limitation which prevents the execution of end-to-end checks daily, it is still possible to perform these checks when both DFRs are triggering on the same transient occurring on the network such as a short-circuit or the opening of a line. The pretrigger period of the records provide indeed an overlapping steady-state. These sections of the records are individually processed by the steady-state integrity checks discussed previously and they are also processed by the end-to-end checks described next.

The idea behind the end-to-end checks is to compare the measured voltage V_R and current I_R at the receiving end of the line with the computed ones deduced from the measured voltage V_S and current I_S at the sending end. To perform these calculations a distributed parameter line model representing the series resistance R', the series inductive reactance X_L' and the shunt capacitive reactance X_C' per unit length is used as illustrated in figure 8. This model is valid even for the longest lines since the charging current is taken into account.

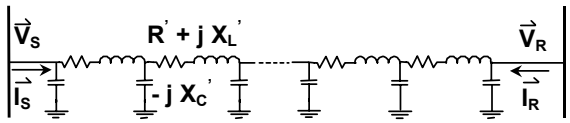

Figure 8: Distributed parameter line model

The equations that relate the voltage V_R and current I_R at one end to the measurements V_S and I_S at the other end are given by:

$$\vec{V}_R = cosh(\gamma L)\cdot\vec{V}_S - Z_c\cdot sinh(\gamma L)\cdot\vec{I}_S \quad (5)$$

$$\vec{I}_R = \frac{1}{Z_C}\cdot sinh(\gamma L)\cdot\vec{V}_S - cosh(\gamma L)\cdot\vec{I}_S \quad (6)$$

The characteristic impedance Z_C and the propagation factor γ are:

$$Z_C = \sqrt{\frac{Z'}{Y'}},\quad \gamma = \sqrt{Z'\cdot Y'} \quad (7)$$

The series impedance per unit length Z' and the shunt admittance per unit length Y' are:

$$Z' = R' + jX_L',\ Y' = j/X_C' \quad (8)$$

Because of the coupling between the phases A, B and C however, the equations (5-6) cannot be used for each phase individually but they apply on the other hand to the decoupled sequence networks. The figure 9 illustrates the positive sequence voltage and current profiles along a 230 kV line which is 315 km long. The profiles computed from V_S and I_S are plotted along the profiles computed from V_R and I_R and these should superpose exactly if perfect measurements and line parameters are used. The step in the voltage near the end of the line is due to a 73 Ohm series capacitor at the remote substation, which is taken into account. These plots highlight the non linear nature of the profiles and emphasize the need to consider the charging current with lightly loaded long lines. It can be observed that the amplitude of the current at one end of the line is about three times the current at the other end in this particular case.

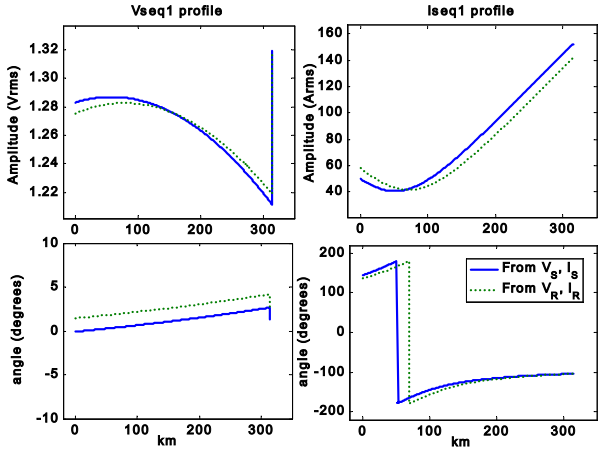

Figure 9: Positive sequence voltage and current profiles

Synchronization issues

With unsynchronized measurements at both ends of the line, the angle of the voltages and currents at one end cannot be checked against the computed one from the other end. However, the relative angle between a voltage and the corresponding current can be checked because the synchronization error then vanishes. This checking allows the detection of some polarity errors and circular permutation errors that cannot be identified easily otherwise as stated before. If the measurements are synchronized with a precise time base such as the GPS for instance, then the individual angles can be compared. A discrepancy between a computed and a measured angle can be attributed to an error into the measurement but it can also reveal an error related to the synchronization process itself. This can happen for example if the time base is transmitted over long distances and the propagation delays are not correctly compensated.

The double-ended fault location algorithms perform systematically end-to-end checks using the prefault period. The computed discrepancy gives an indication of the integrity and the quality of the measurements. It contributes also to the estimation of an error margin given with the result that is based on empirical rules. This practice allowed the detection of currents with bad scaling among other things. In one case, the software reported a 30% discrepancy in the prefault currents. After a short verification it was found that a full scale primary current was specified as being 35 kA instead of 45 kA. After having corrected this error the fault location estimate given to the patrollers led them right to the span responsible for the permanent fault on this line 378 km long. The conductors of the two faulted phases were found twisted together. This unusual event was attributed to wet snow and high winds prevailing when the fault occurred. Another cause for end-to-end discrepancies is a wrong assumption about the status of shunt inductances, which is given by Sequence of Event Recorders (SERs). Since the inductances are situated on the line side relative to the CT, their current must be deduced from the voltage measurement and then subtracted from the CT measurement to obtain the true current of the line.

V. Transient-state integrity checks

This section proposes some integrity checks to be performed with transient-state classified signals.

V.1 Kirchoff's current law verification

The Kirchoff's current law states that the sum of all the currents going in and out of a node should balance to zero. The following example shows how the application of this law permits to detect error measurements. The figure 10 illustrates a series capacitor with its related protection. A DFR measures the line current and another one measures the current in the capacitor branch *I_Cap*, the current in the varistor branch *I_Var* and the current in the spark gap branch *I_Gap*. The three parallel branches should add up to be equal to the line current. The application of this law with a real-life short-circuit event revealed some errors into the measurements. A first error was noticed in the gain of all the current measurements of the DFR supervising the series capacitor. They all presented a gain too low by a sqrt(2) factor. This is a relic of an old habit that some people had when using the light beam oscillographs. The modified gain allowed them to obtain the rms value of a sinusoidal signal simply by reading the crest value. After the correction of this gain by software there still

exists a large discrepancy when the sum of the branch currents are superposed over the line current as shown in the upper part of figure 11. The lower part of the figure shows the error signal obtained by subtracting one signal from the other. The cause of this error is not found yet although the susceptibility to interference when the spark gap flashes is one hypothesis.

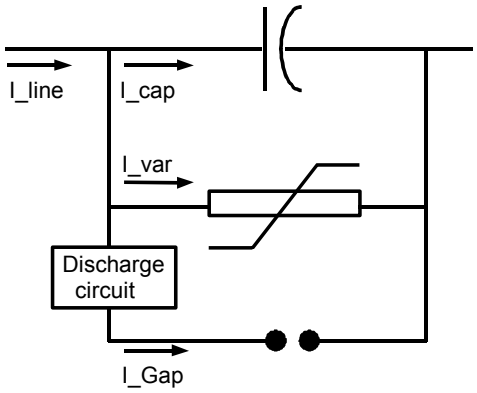

Figure 10: Series capacitor's current measurements

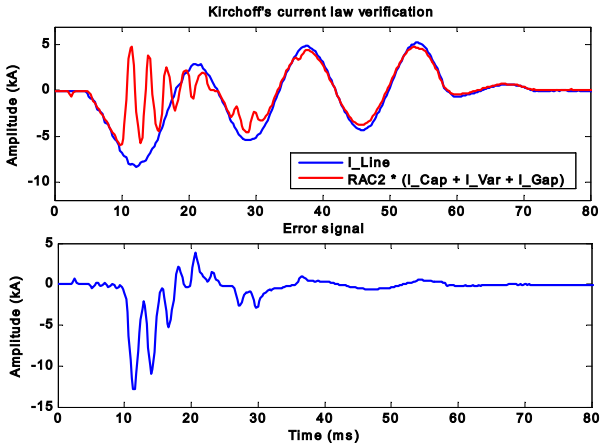

Figure 11: Kirchoff's current law verification reveals two errors

Another application of the Kirchoff's current law is possible if the neutral current of a line is measured in addition to the three phase currents. The figure 12 illustrates a case where the negative of these three currents didn't add up to equal the neutral current. A perfect multiplying factor of –3 existed between the two. It was found that the neutral current was not really measured but it was rather computed from the line currents. An error was introduced in the equation because the zero sequence current Iseq0 = 1/3·(Ia+Ib+Ic) was confused with the neutral current In = –(Ia+Ib+Ic). This kind of error may lead to misinterpretation if the wrong neutral current is used with a transient waveform playback system to test a protective relay for instance.

One more interesting case is related to the catastrophic failure of a CT, which exploded two years ago. The upper part of figure 13 illustrates the fault voltage and the lower part shows one of the line currents.

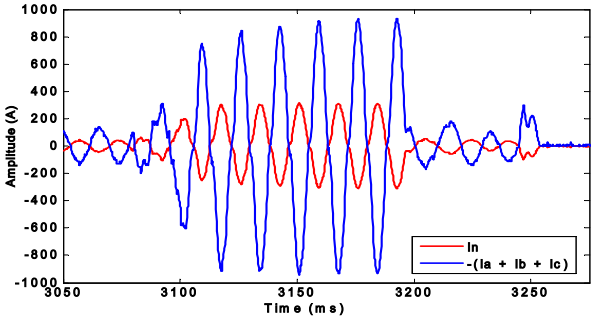

Figure 12: Kirchoff's current law verification reveals an error

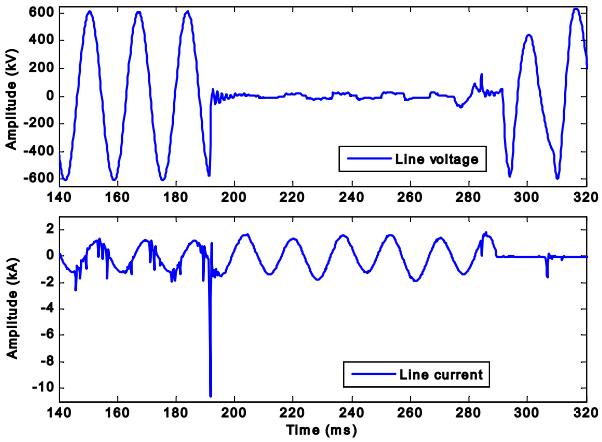

Figure 13: Noise in the prefault line current prior to the explosion of the CT

It can be observed that the prefault voltage is sound but the prefault current seems very noisy. The high noise affected in fact many current measurements from different lines.

A closer look given in the upper part of figure 14 shows that the notches and spikes affect the three phases in a common mode. A Kirchoff's current law verification is made by comparing the measured neutral current of the line with the computed negative sum of the three phase currents. The plot of this computed neutral current in the lower part of figure 14 confirms that the noise adds up in a common mode. Moreover, the superposition over the measured neutral current proves that this noise was in fact not really present at the primary side of the CTs. It was rather induced into the measurements in all likelihood as a result of arcing inside the CT prior to the explosion. The figure 15 shows a picture of the remains of the CT. The question is whether the explosion could have been prevented if the daily checks had been implemented then. The previous record taken by the DFR four days before the incident is showing no sign of anomaly. This suggests that such degradation occurs rapidly and it demands a fast intervention.

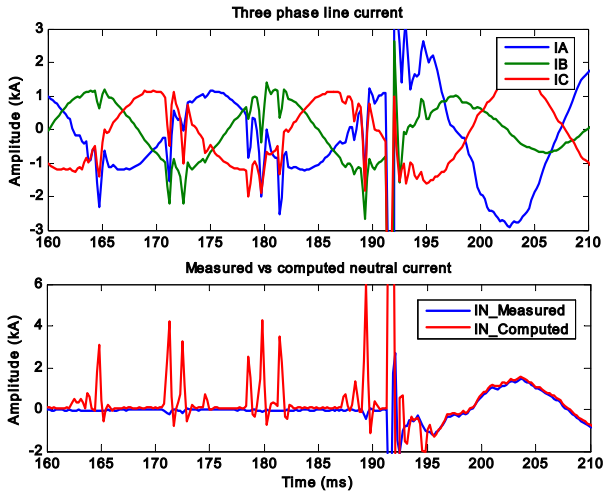

Figure 14: Closer look at the prefault currents and verification of the Kirchoff's current law

Figure 15: Picture of the remains of the CT

V.2 Redundant instantaneous voltage checks

In section IV dedicated to steady-state checks it was proposed to compare the fundamental component of the redundant voltages against each other. In this section it is proposed to compare the instantaneous redundant voltages in the time domain to detect errors in transient-state. The figure 16 illustrates three redundant line voltages measured during a sectionalizer fault at the substation. Two measurements come from capacitive coupling voltage transformers (labelled 'CCVT 1' and 'CCVT 2') and the other comes from a magnetically coupled voltage transformer (labelled 'MCVT'). The three voltages superpose quite well in the prefault period. However, the CCVT 2 associated with the faulted line shows a large discrepancy relative to the others during the fault period. This was due to the combined effect of ground potential rise with bad grounding of the measurement cables. Because of this error the fault location algorithm sensed the fault in the reverse direction. When using one of the two sound voltages the algorithm was giving a close estimate of 500 meters in the forward direction. In two similar cases not shown here, the bad grounding has caused a 10 km error in the fault location estimate. When using a sound redundant voltage, the error was reduced to a few hundred meters for lines that measure over 200 km in both cases.

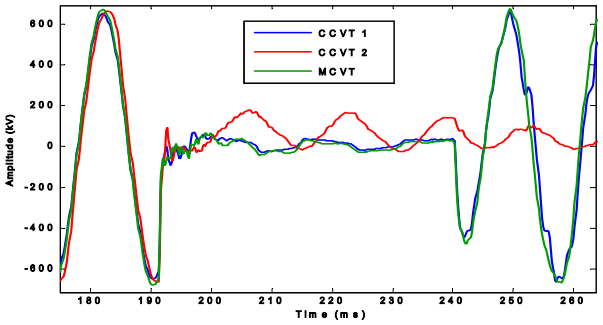

Figure 16: Effect of bad grounding during a fault

The figure 17 shows another kind of voltage measurement error revealed only during a transient-state. Two voltages superpose very well and a third one exhibits huge oscillations reaching up to 2 p.u.. A defective anti-resonant circuit into the CCVT was found responsible for this apparent overvoltage, which provoked the tripping of the line by an overvoltage relay.

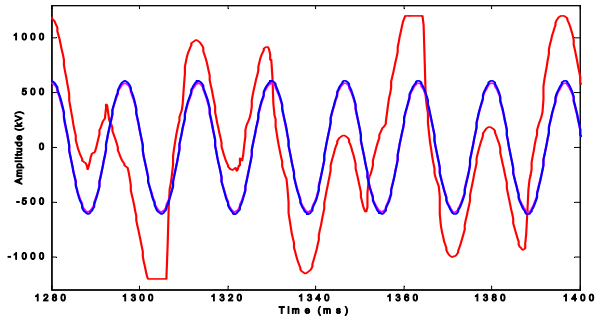

Figure 17: Defective anti-ferroresonance circuit of a CCVT

V.3 Checking for other anomalies

There is other kind of anomalies in transient-state that may be detected automatically. The figure 18 illustrates the current measurement of a faulted phase and the neutral current during a switch onto fault. Both signals exceeded their full scale limit. This situation can be easily detected by verifying that each sample value remains below its maximum A/D value.

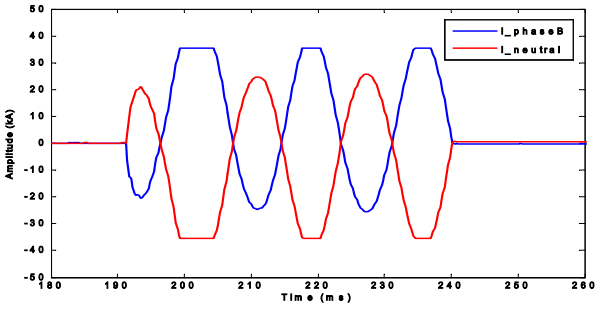

Figure 18: Faulted phase and neutral currents exceeding their full scale limit

The upper part of figure 19 illustrates one more example of an error in a current measurement discovered only in transient-state. The recording shows that during a fault the

current switches suddenly from a negative value to a positive value momentarily. This strange behaviour was attributed to a software bug of the DFR inside a function performing temperature compensation. When the amplitude reached the full scale limit during the fault the few counts that were added up for compensation caused a register to overflow. A function was developed to correct the corrupted signals afterwards and the resulting signal is shown in the lower part of the figure.

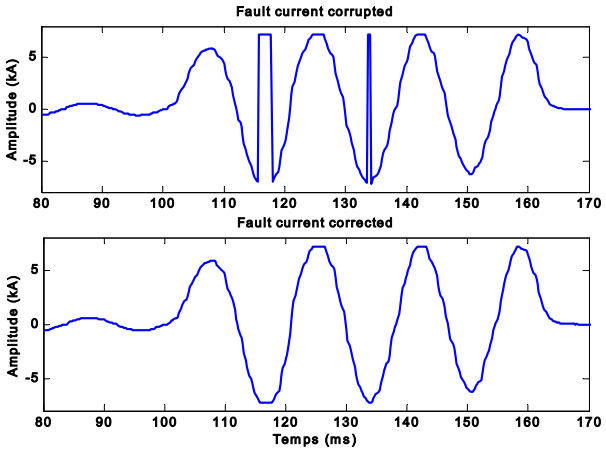

Figure 19: Fault current corrupted by a software bug before and after the correction

The detection of the saturation of the CTs and a mean to correct it afterwards certainly also deserves attention. However, these problems are not common at Hydro-Québec owing to the specifications demanded and many references to good papers may be found in the literature**.**

VI. Cross-checking with other IEDs

It is proposed to extend the approach presented in the previous sections to include other IEDs such as the digital protective relays, the Phasor Measurement Units (PMUs), the Power Quality meters and the SERs for instance. The benefits proved to be so valuable for the DFR system that the idea of cross-checking their measurements against other IEDs seems very attractive. The sharing of information from different devices may turns out to be much more advantageous than one might expect at first sight. It was shown in section IV that the redundant voltage measurement checks using a DFR for instance does not permit to discriminate between an error owing to the voltage transformer and an error owing to the DFR system. The comparison of measurements extracted from independent devices would allow eliminating this uncertainty regarding the source of the error. Another great advantage of polling the IEDs regularly would be to verify their availability, as it was proposed for the DFRs.

One subject, which draws much attention in these days, is the implication of the protective relays in the cascade of events leading to major blackouts [2]. They appear to contribute to the cascade of events in about 75% of the cases [3]. The main cause for this is the hidden failures into the protective systems that remain unnoticed until a disturbance reveals the defects. The automated checking of the relay inputs in service against redundant measurements on a regular basis would guarantee their health and would allow the early detection of some hidden failures. Moreover, the recurrence of problems with bad scaling, bad PT or CT ratios and wrong signal assignment would be greatly reduced. The blackout that struck South London in UK the August 28th 2003 [4] would have been avoided for instance. The culprit responsible for the cascading event was a 1 ampere rated relay which was installed instead of the 5 amperes relay specified. Because of this error the relay was reading a current five times higher than in reality. Hydro-Québec has also experienced an erroneous tripping of a line because of a wrong reading by a relay with a bad CT ratio. The tripping at an untimely moment participated in the cascade of events leading to the loss of an entire 735 kV substation. Furthermore, the checking of the inputs of the digital relays by redundant measurements could lead to a questioning about the necessity to test them with amplifiers in routine maintenance.

Regarding the synchronization issues between the measurements, it would be useful if the IEDs could freeze a measurement at a moment programmed in advance in order to compare readings taken simultaneously. Another solution would be to use a relay with synchrophasor capability. The readings would then be continuously transmitted with a time tag associated that would facilitate the comparison of simultaneous readings. The checking against the PMUs measurements would also provide the same benefits.

The checking could also include the SERs to cross-check the status of the breakers and the sectionalizers for instance. A wrong network topology assumption might induce large errors in the results of state estimators.

VII. Conclusion

Many real-life examples of errors into the DFR's measurements have been given in this paper to share the experience of Hydro-Québec gained from the fault location application over the last few years. A new approach has been proposed to improve the reliability of the DFR system by forcing a recording daily and performing some automated integrity checks on the measurements. The approach implemented last year already proved its usefulness after just a few months of operation. It raises the confidence towards the automated sending of fault location estimate by email implemented this year. In a recent event, a fault location estimate was sent automatically by email to the field personnel four minutes after the occurrence of a fault on a line 100 km long. The patrollers sent by snowmobiles located a broken insulator string four towers beside the given estimate.

A demonstration project aiming to cross-check the DFR's measurements with other IEDs is in its starting phase at Hydro-Québec. In the long term, it is anticipated that it will be possible to perform the proposed integrity checks on a near continuous basis given the capabilities of future IEDs. The expected improvements in communications within the substations and the better interoperability across systems will facilitate further the adoption of this philosophy. The ultimate goal is to detect hidden failures earlier and consequently improve the reliability of the power systems.

VIII. References

[1] C. Fecteau, D. Larose, C. Deguire, Nouveaux Algorithmes de localisation de défauts et expérience sur le réseau de transport d'Hydro-Québec (in French), CIGRÉ Study Committee B5 Colloquium, Sept. 30-Oct. 1, 2003, Sydney, Australia.

[2] J. Chen, J. S. Thorp, I. Dobson, Cascading Dynamics and Mitigation Assessment in Power Disturbances via a Hidden Failure Model, Intl. Journal of Electrical Power and Energy Systems, 2003.

[3] A. G. Phadke, J. S. Thorp, Expose Hidden Failures to Prevent Cascading Outages, IEEE Computer Applications in Power, July 1996, pp. 20-23.

[4] IEE, Tracing the London Blackout, IEE Power Engineer, Vol. 17, No. 5, Oct.-Nov. 2003, pp. 8-9.

IX. Biographies

Claude Fecteau was born in Montreal, Canada, in 1963. He obtained his B.A.Sc. and M.A.Sc. degrees in electrical engineering from École Polytechnique, Université de Montréal, in 1986 and 1989 respectively. His Master's thesis described one of the first operational PC-based transient waveform playback system for testing protective relays. He joined Hydro-Québec in 1989 as a research engineer at the IREQ research institute where he continued the development of the relay test system known as "SERA-NewWave PC-playback system". He also developed the software of a digital fault recorder. He invented new fault location algorithms, which are being used extensively at Hydro-Québec. His main interests are signal processing, protection, fault location and reliability. He is a member of the IEEE Power Engineering Society and Standard Association.

Denis Larose was born in Barraute, Canada, in 1954. He obtained a College Diploma (DEC) in Electrotechnics from the Collège Ahuntsic in 1977. He joined the Canadian Standards Association in 1977 as a Laboratory Technician where he was involved in the testing of industrial equipments. In 1979, he joined Hydro-Québec as an Analyst of the protection systems behaviour in the Control and Protection department of TransÉnergie. He is also responsible for the maintenance of a database used for the compilation of statistics about the performance of the protection systems and the reliability of the power network. He is involved in the specification of software requirements for the automated analysis of protection systems and DFR's records.

Raymond Bégin obtained his B.A.Sc. in electrical engineering from Laval University in Québec, in 1977. He works at Hydro-Québec since 1979. From 1979 to 1985, he worked on the certification of protective relays dedicated to the bulk power network and he also provided the related technical support to other employees. Since 1990, he is responsible for the analysis of the protective relay and special protection system operations in the Control and Protection department of TransÉnergie. During the same period, he developed an expert system (SAME) for the automated analysis of the performance of the protection systems. He is an active member of the Order of Engineers in the province of Québec.